A μ-Rhythm Matched Filter for Continuous Control of a Brain-Computer Interface

Dean J. Krusienski*, *Member, IEEE*, Gerwin Schalk, *Member, IEEE*, Dennis J. McFarland, and Jonathan R. Wolpaw

Abstract—A brain-computer interface (BCI) is a system that provides an alternate nonmuscular communication/control channel for individuals with severe neuromuscular disabilities. With proper training, individuals can learn to modulate the amplitude of specific electroencephalographic (EEG) components (e.g., the 8–12 Hz μ rhythm and 18-26 Hz β rhythm) over the sensorimotor cortex and use them to control a cursor on a computer screen. Conventional spectral techniques for monitoring the continuous amplitude fluctuations fail to capture essential amplitude/phase relationships of the μ and β rhythms in a compact fashion and, therefore, are suboptimal. By extracting the characteristic μ rhythm for a user, the exact morphology can be characterized and exploited as a matched filter. A simple, parameterized model for the characteristic μ rhythm is proposed and its effectiveness as a matched filter is examined online for a one-dimensional cursor control task. The results suggest that amplitude/phase coupling exists between the μ and β bands during event-related desynchronization, and that an appropriate matched filter can provide improved performance.

Index Terms—Brain-computer interface, electroencephalogram, matched filter, sensorimotor rhythms, spectral analysis.

I. INTRODUCTION

A Brain-Computer Interface (BCI) is a system that allows individuals with severe neuromuscular disabilities to communicate or perform ordinary tasks exclusively via brain waves [18]. A BCI monitors brain activity either invasively or noninvasively [i.e., electroencephalographic (EEG) activity] and translates predetermined features, corresponding to the user's intentions, into device commands. The first step in developing a successful noninvasive BCI paradigm is determining suitable control features from the EEG. An effective control signal has the following attributes: it can be precisely characterized in an individual user, it can be readily modulated by the user according to intent, it can be detected and tracked consistently and reliably, and it can be readily translated into device control. Standard control signals used for noninvasive BCIs fall under two basic categories: stimulus evoked potentials and event-related (de)synchronizations [11]. Stimulus evoked potentials are phase-locked to the stimulus; however, they are discrete responses that cannot easily be modulated for continuous control. On the other hand, event related (de)synchronizations are

responses that can attenuate or intensify in a continuous fashion in response to a stimulus or event and hence are well suited for real-time control. The cortical μ rhythm is an example of an event-related desynchronization that is commonly used as a control feature for BCIs.

A. The Cortical μ Rhythm

The cortical μ rhythm is an idling rhythm that is evident in the scalp recorded EEG of most healthy adults [13]. It is prominent over the primary sensorimotor cortical areas and is generally characterized by an arch-shaped 8–12 Hz rhythmical pattern, as depicted in Fig. 1. The μ rhythm is typically suppressed by contralateral movement, tactile stimulation, and movement imagery. The foci of the responses over the left and right hemispheres are not synchronous, but the relative amplitude fluctuations can be correlated as a result of jointly dependent sensorimotor activity. With adequate training, an individual can develop significant control over the independent μ-rhythm modulation for each hemisphere, as demonstrated in [6]. Because of similar localization and activation patterns, the β rhythm is thought to be related to the μ rhythm, but the exact relation remains uncertain. A study of the general phase synchronization between α and β rhythms in the EEG, not specific to the cortical μ rhythm, can be found in [12]. This study suggests that significant α-synchronous β oscillations exist, which may not be simple proportional-amplitude harmonics.

B. Conventional Spectral Detection and Tracking

As specified earlier, two of the keys to realizing an effective BCI control signal are precise characterization and reliable detection of the signal. The μ rhythm is commonly identified by its distinctive arch-shaped morphology, but the presence of this morphology in on-line recording is often obscured by noise. Because of its characteristic 8-12 Hz spectral band, spectral analysis methods that resolve sinusoidal components such as Fourier based methods [1], autoregressive (AR) models [3], and narrow-band power estimation [4] are the traditional techniques employed for continuous tracking of the μ rhythm in BCIs. Although these spectral methods are efficient and often effective in this context, there are several fundamental problems with these approaches. Firstly, the visual α-rhythm is prominent in normal EEG and occupies the same frequency band as the μ rhythm. Although the visual α-rhythm is typically most prominent in the occipital regions, it can also be present over the sensorimotor cortex [11]. The influence of visual α-rhythm over the sensorimotor cortex can be diminished via spatial filtering such as the large Laplacian, but often is not totally eliminated. Although the visual α-rhythm is usually more sinusoidal than the μ rhythm, it is often difficult to discriminate the two rhythms using spectral

*D. J. Krusienski is with the University of North Florida, Jacksonville, FL 32224 USA (e-mail: deankrusienski@ieee.org).

G. Schalk, D. J. McFarland, and J. R. Wolpaw are with the Wadsworth Center, New York State Department of Health, Albany, NY 12201 USA.
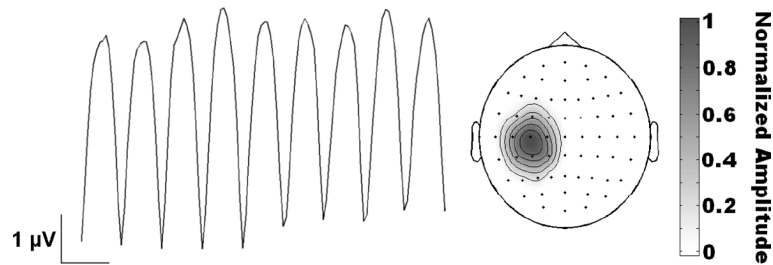
Fig. 1. Prototypical μ-rhythm temporal waveform and the unit normalized amplitude topography over the hand area of the sensorimotor cortex for right hand imagery.
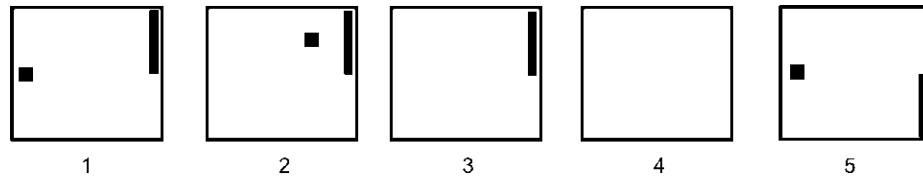

Fig. 2. One-dimensional task trial structure. (1) The target and cursor are present on the screen for 1 s. (2) The cursor moves steadily across the screen for 2 s with its vertical movement controlled by the user. (3) If the user hits the target, the target flashes for 1.5 s. If the cursor misses the target, the screen is blank for 1.5 s. (4) The screen goes blank for a 1-s interval. (5) The next trial begins.

amplitude information alone. Another drawback of traditional spectral estimation techniques is that they are incapable of compactly and accurately modeling the sharp, peaking discontinuities characteristic of the μ rhythm. Such spectral techniques are not explicitly conducive to tracking phase-coupled components and are typically not configured to include phase information.

These issues can be addressed by harnessing the characteristic μ-rhythm morphology for a particular user and exploiting it as a template for a matched filter analysis. Matched filters [17] are known to be particularly effective for detection of waveforms with consistent temporal characteristics in the presence of noise, such as the sinus rhythm in the electrocardiogram, for instance.

II. METHODOLOGY

In one- and two-dimensional cursor control studies [9], [10], [19], [20], trained users are able to effectively modulate 8–12 Hz (μ band) and 18-26 Hz (β band) spectral components over the sensorimotor cortex to move a cursor toward a randomly positioned target on a monitor. In order to investigate the nature of the μ rhythm for a particular user, the characteristics of the μ-rhythm were examined using data from 11 able-bodied users (6 women and 5 men ranging in age from 29-45). All users had exhibited strong μ-band activity during an initial screening and were subsequently trained on a simple two-target, one-dimensional cursor control task. All users were successfully trained on the task (consistently $> 80\%$ accuracy) and ranged in experience from 1 to 20 sessions on the task prior to this data set. The study was approved by the New York State Department of Health Institutional Review Board, and each user gave informed consent.

A. One-Dimensional Cursor Control Task

The one-dimensional sensorimotor rhythm cursor control task is shown in Fig. 2. For the task, the users were presented with a target randomly positioned at the top or bottom of the

right edge of the monitor. The trial began with the cursor at the center of the left edge of the monitor. It moved at a constant rate toward the right, reaching the right side of the monitor after 2 s. The users' goal was to move the cursor upward or downward to the height of the target so that it hit the target when it reached the right side of the monitor. The trials continued in 3-min runs, with a 1-min break given between runs. A single 3-min run consisted of between 18 and 30 trails, and 8 runs constituted a single session. Sessions were conducted one per day, two or three times a week over a period of several weeks.

B. Data Collection and Feature Extraction

The details of the data collection and analysis are as follows: Using BCI2000 software [15], the EEG activity was collected from 64 channels at standard locations [16] distributed over the scalp. All 64 channels were referenced to the right ear, bandpass filtered (0.1–60 Hz) and digitized at 160 Hz. A large Laplacian spatial filter [8] was applied to the electrode over the right or left hand area of the sensorimotor cortex that was predetermined as optimal for each user based on analysis of prior sessions (see Table I). For each user, a 3-Hz bin at a predetermined fundamental frequency from a 16th-order AR model was extracted from the spatial-filtered signal and used as the online control feature. The AR feature was calculated every 50 ms from the past 400 ms of data.

C. Characteristic μ Rhythm

The first step toward extracting the characteristic μ-rhythm waveshape for a particular user was the determination of the spectral component over the sensorimotor cortex that demonstrated the highest correlation with the target location. This was accomplished using features generated by a 16th-order AR model, although any adequate spectral technique would presumably suffice for this step. This spectral component was assumed to be the fundamental frequency of the user's μ rhythm. Next, data from each 2-s trial for the target location that

TABLE I
AMPLITUDE /PHASE RELATIONSHIPS

User	Location	Freq. (Hz)	$a_2/a_1 : a_3/a_1$	$\phi_2 : \phi_3$ (rad)
A	C_3	12	0.29 : 0.05	1.75 : 4.41
B	C_3	12	0.19 : 0.03	3.30 : 0.61
C	C_{P3}	12	0.09 : 0.01	2.83 : 6.11
D	C_3	12	0.27 : 0.06	3.64 : 0.72
E	C_{P3}	11	0.06 : 0.02	3.99 : 1.46
F	C_3	12	0.17 : 0.03	3.33 : 0.38
G	C_4	12	0.12 : 0.02	3.39 : 0.71
H	C_{P4}	13	0.13 : 0.02	1.89 : 5.65
I	C_3	12	0.50 : 0.09	3.80 : 0.60
J	C_3	12	0.15 : 0.02	3.10 : 1.08
K	C_3	10	0.16 : 0.03	3.78 : 1.13

For each of the 11 users, the predetermined optimal electrode location (International 10–20 System) and fundamental μ-rhythm frequency, the ratio of amplitudes of the first two harmonic peaks (a_2 and a_3), and the fundamental μ peak amplitude (a_1) of the characteristic waveform, and phases of the first two harmonics (ϕ_2 and ϕ_3) of the characteristic waveform relative to zero-phase of the fundamental μ component ($\phi_1 = 0$) are listed.
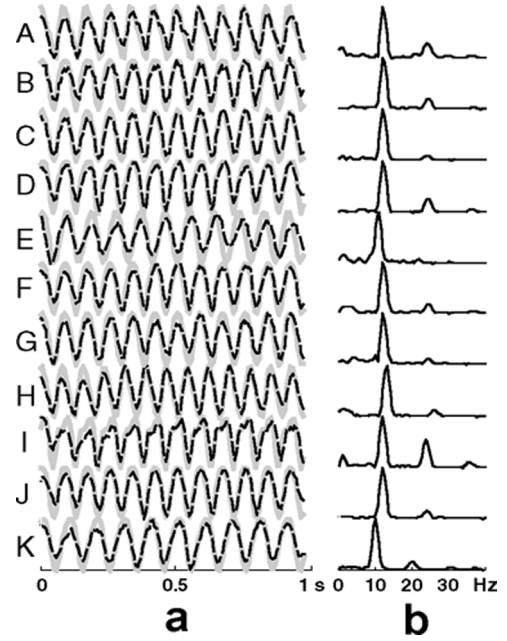

Fig. 3. Normalized characteristic waverforms and the corresponding FFT amplitude spectra for the 11 users: (a) The averaged characteristic waveform (dashed) versus parameterized μ-rhythm template (solid). (b) FFT amplitude spectra of the characteristic waveforms.

TABLE II
STRENGTH OF SYNCHRONIZATION (TOP /BOTTOM TARGET)

User	S_{12}	S_{13}
A	0.23 / 0.05	0.12 / 0.02
B	0.31 / 0.15	0.11 / 0.04
C	0.23 / 0.09	0.05 / 0.02
D	0.40 / 0.08	0.13 / 0.01
E	0.20 / 0.05	0.07 / 0.01
F	0.43 / 0.02	0.21 / 0.03
G	0.45 / 0.14	0.11 / 0.02
H	0.30 / 0.08	0.06 / 0.01
I	0.35 / 0.08	0.20 / 0.04
J	0.55 / 0.33	0.16 / 0.10
K	0.32 / 0.09	0.10 / 0.03

For each of the 11 users, the strength of synchronization (2) between the fundamental frequency and the first harmonic (S_{12}) and the fundamental frequency and the second harmonic (S_{13}) for the two target conditions are listed.

corresponded to μ-rhythm synchronization was cross-correlated with a 1-s sinusoid template at the fundamental frequency. The 1-s segments having the maximum correlation for each trial were collected over two entire sessions of data. These phase aligned data segments were then averaged to expose the prevailing characteristics of the control signal.

The averaging revealed distinctive characteristic μ-rhythm morphologies, which are depicted in Fig. 3(a). It is evident that all of the waveforms are nonsinusoidal and periodic, and that several of the users's characteristic waveforms resemble the classical arch shape.

Although the μ rhythm typically tends to appear in bursts lasting anywhere from less than 1 s to several seconds, the averaged waveforms maintain a relatively constant amplitude envelope during the 1-s interval. Because of this constant envelope and because no significant temporal variations were evident, other than that attributed to noise, it is feasible to derive a parameterized model of the μ rhythm that could be easily applied as a matched filter template.

D. Paramaterized μ-Rhythm Model

The fact that the characteristic μ-rhythm waveforms exhibit periodicity indicates that it can be decomposed in terms of a discrete number of phase-coupled sinusoidal components. In order to develop a model for the parameterized μ-rhythm templates, the Fourier spectra of the characteristic waveforms were examined using the fast Fourier transform (FFT).

Fig. 3(b) depicts the spectra of the characteristic waveforms given in Fig. 3(a). It is observed that the magnitude spectra primarily consist of a principal peak at the fundamental frequency and one or two decaying harmonic peaks. The exact relationships of these harmonics as determined by magnitude and phase components of the FFT are given for each user in Table I. Table I lists the ratio of amplitudes of the first two harmonic peaks (a_2 and a_3) and the fundamental μ peak amplitude (a_1), and phases of the first two harmonics (ϕ_2 and ϕ_3) relative to zero-phase of the fundamental μ component ($\phi_1 = 0$). Because the harmonic

phases are proportionally related, they can easily be converted into the cyclic relative phase

$$\psi_{uv}(t) = \left(\frac{v}{u} \phi_u(t) - \phi_v(t) \right) \bmod 2\pi, \text{ with } \mu > v \qquad (1)$$

and the strength of synchronization [14]

$$S_{uv} = \left| \frac{1}{N} \sum_{t=1}^{N} e^{j\psi_{uv}(t)} \right| \qquad (2)$$

where N is the number of instantaneous phase observations over an interval. Ideally, if there is no phase coupling between harmonics, the relative phase should have a uniform random distribution and the strength of synchronization will equal zero. Table II lists, for each of the 11 users, the strength of synchronization between the fundamental frequency and first harmonic (S_{12}) and the fundamental frequency and second harmonic (S_{13})
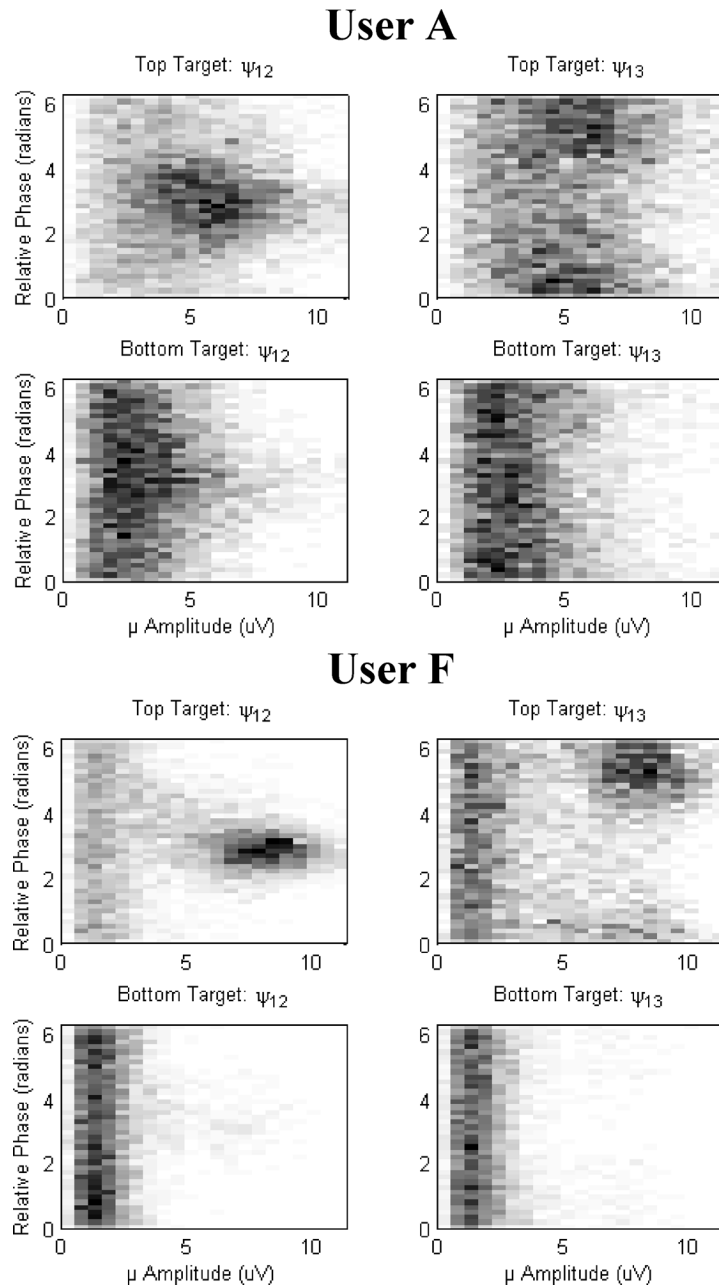
Fig. 4. Two-dimensional histograms of relative phase versus μ-band amplitude for two representative users. Increasing density of observations is indicated by increasing darkness. The users are desynchronizing the μ rhythm for the bottom target and synchronizing it for the top target. The uniform distributions with respect to amplitude for the bottom target indicates that there is little phase coupling when the μ rhythm is desynchronized. Conversely, there is specific amplitude and phase concentration for the top target when the μ rhythm is synchronized.

for the two target conditions. There is clearly a stronger synchronization between the fundamental frequency and the first two harmonics for the top target trials compared to the bottom target trials. A paired t-test on the strength of synchronization indicates a significant difference ($p < 0.0001$) between target conditions for both S_{12} and. S_{13}. Furthermore, the phase relationships are dependent upon the signal amplitudes. Two-dimensional histograms of the relationship between the relative phase and the μ-rhythm amplitude for the two target positions are illustrated in Fig. 4 for two representative users. The users are desynchronizing the μ rhythm for the bottom target and synchronizing it for the top target. The uniform distributions with

respect to amplitude for the bottom target indicates that there is little phase coupling when the μ rhythm is desynchronized. Conversely, there is specific amplitude and phase concentration for the top target when the μ rhythm is synchronized.

These results indicate that, during specific sensorimotor cortex activity associated with control, the harmonic components of the μ band are consistently phase-coupled. Considering this, combining the μ and β bands as independent control features for a BCI is likely suboptimal in terms of detection and tracking performance. This underscores the need for a feature extraction method that is capable of compactly modeling the amplitude and phase interdependencies among frequency

bands for more accurate detection and tracking of control signal modulation. These issues can be addressed by constructing a suitable matched filtering scheme based on the empirically derived characteristic waveform.

Neglecting the noise characteristic, a general matched filter template that maximizes the signal-to-noise ratio [17] is simply modeled as a sum of the harmonically related sinusoidal components

$$MF(n) = \sum_{k=1}^{N} a_k \cos\left(\frac{2\pi n k f_F}{f_S} + \phi_k\right) \qquad (3)$$

where n is the template sample number, f_S is the sampling frequency, f_F is the fundamental frequency of the μ-rhythm template, $N - 1$ is the number of harmonics to be modeled, and a_k and ϕ_k are the amplitude and phase of the individual harmonics, respectively. These model parameters are simply obtained from the FFT spectrum of the user's characteristic waveform as given in Table I, with $N = 3$ sufficient for modeling the characteristic μ rhythm. The resulting template waveforms corresponding to the individual characteristic waveforms are illustrated in Fig. 3(a). Since much of the EEG is comprised of quasi-periodic or quasi-sinusoidal signals characterized by coupled, harmonically related frequencies, this model is capable of compactly representing for detection purposes a plethora of EEG signals such as steady-state visual evoked potentials (SSVEPs). An alternate, less general model of the μ rhythm using a single rectified and shaped sinusoid is provided in [5].

E. Paramaterized μ-Rhythm Matched Filter

To use the μ-rhythm template waveform generated by the parameterized model [see Fig. 3(a)] as a matched filter, an appropriate segment length was selected according to the desired update rate (see Section III). The μ-rhythm template waveform segment was then normalized to unit amplitude. The incoming data segments, having segment length equal to the template waveform, were circularly convolved for one period of the template in order to evaluate the template at discrete phase shifts, essentially determining the optimal phase correlation between the data segment and the template. This is equivalent to an FIR filter bank of f_S/f_F phase shifted template waveforms, though it is realistic to use a smaller subset of shifts at high sampling rates. The square root of the maximum value of the circular convolution (or maximum filter bank output), corresponding to the optimal alignment, was taken to be the feature for the data segment. The result is a continuous amplitude analysis, similar to that produced by a single frequency bin of a conventional spectral analysis technique.

III. OFFLINE ANALYSIS

To evaluate the performance of the parameterized μ-rhythm template as a matched filter for tracking actual coordinated μ-rhythm modulations, the results were assessed against three comparable spectral estimation techniques for offline analysis of the one-dimensional cursor control task described in Section II-A. The data set used for offline analysis, collected as described in Section II-B, consisted of 4 sessions of 8 runs each from each of the 11 users. These 4 test sessions were subsequent to those sessions used to generate the matched-filter (MF) templates for validation purposes. For the offline analysis, the features were calculated every 50 ms using 400 ms of data via the following techniques.

AR1: The incumbent online method using a 16th-order AR model derived via the maximum entropy method (MEM) [7], with a single 3-Hz bin in the μ band.

AR2: A 16th-order AR model derived using the maximum entropy method (MEM) [7], with 1-Hz bins in the μ and β bands.

FFT: A 160-point FFT (zero padded) with a Hamming window applied to the data, with 1-Hz bins in the μ and β bands.

MF: The individualized μ-matched filter in the μ band using (3) and the parameters given in Table I.

The frequency bins were chosen to be relatively narrow to provide a more objective comparison to the fundamental frequency of the μ-matched filter templates. The frequency bin corresponding to the fundamental μ-band frequency and the bin at twice the fundamental frequency (β band) were selected to compose the control features from the spatial filtered channel. The AR2 and FFT methods were chosen in order to examine the relative effects of disregarding phase-coupling between the μ and β bands.

The optimum linear regression coefficients for the features generated by each technique were determined to predict the vertical target location for each session. The equation expressing the instantaneous vertical output prediction is given as follows:

$$\Delta_{predicted} = w_\mu A_\mu + w_\beta A_\beta + b. \qquad (4)$$

The terms w_μ, w_β, and b are the optimal regression coefficients for the μ and β spectral amplitude features, A_μ and A_β, respectively. The three regression coefficients (μ, β, and intercept) were determined for both the FFT and AR2 models, and only two coefficients (μ and intercept) were determined for the AR1 and MF methods, since the β activity is assumed to be inherent in the features generated by the matched filter.

The predictions generated by the linearly weighted features were then averaged for each trial and correlated with the respective vertical target locations. The results obtained from the four techniques are summarized in Fig. 5, where each bar indicates the average r^2 (i.e., the proportion of the variance of the EEG signal for top and bottom targets accounted for by target position) for the 11 users. A repeated measures analysis of variance (ANOVA) was conducted on the offline session results using METHODS, USERS, and SESSIONS as factors. The ANOVA revealed a significant difference between the methods ($F(3, 30) = 3.63$, p $= 0.0148$). Although the MF consistently resulted in the best performance, a posthoc Tukey-Kramer test only revealed a significant difference between AR1 and MF (p < 0.05). There was not a significant difference in the interaction of user and method ($F(30, 300) = 0.33$, p $= 0.9996$), indicating that the difference in methods was consistent across users.
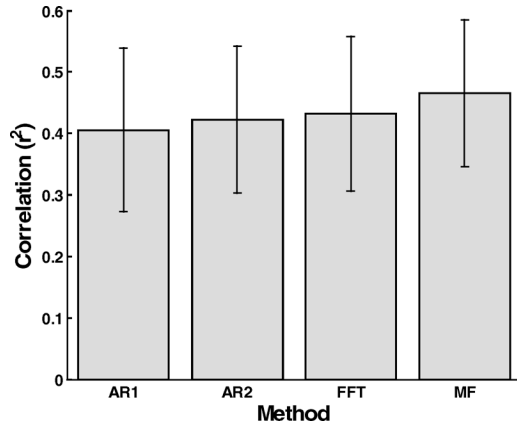
Fig. 5. Results of the offline analysis comparing the four feature extraction methods. Each bar indicates the trial-averaged r^2 (i.e., the proportion of the variance of the EEG signal for top and bottom targets accounted for by target position), averaged across the 11 users. The error bars indicate standard deviation. ANOVA results indicate that the difference between methods is consistent.

TABLE III
AVERAGE CONTROL FEATURE SKEWNESS AND KURTOSIS ACROSS 11 USERS
FOR THE TWO TARGET LOCATIONS

	Top Target		Bottom Target	
	Skewness	**Kurtosis**	**Skewness**	**Kurtosis**
AR1	0.72 ± 0.39	3.20 ± 1.05	1.85 ± 0.87	9.18 ± 6.75
AR2	1.18 ± 0.32	4.67 ± 1.39	2.26 ± 1.17	13.11 ± 11.02
FFT	0.60 ± 0.38	3.08 ± 0.83	1.54 ± 0.93	8.95 ± 9.02
MF	-0.02 ± 0.31	2.43 ± 0.47	0.56 ± 0.45	3.74 ± 1.37

For continuous cursor control, it is desirable that the control feature distribution be symmetric. A skewed control feature distribution not only makes it more difficult to estimate the mean of the features, but also biases the cursor toward a particular target despite articulated signal modulation. Additionally, a skewed distribution affects the speed and directional tendencies of the cursor, which can be distracting to the user. To account for this, the skewness of the control feature distribution can be determined. Skewness, the third central moment, is a measure of the asymmetry of the data around the sample mean. If skewness is negative, the data are spread out more toward the negative side of the mean than to the positive. If skewness is positive, the data are spread out more toward the positive side of the mean. The skewness of a perfectly symmetric distribution is zero.

Optimization of the feature weights for the online cursor update is performed using ordinary least squares linear regression. Because ordinary least squares linear regression is optimal under the assumption of Gaussianity, it is also desirable that the control features have a Gaussian distribution. Kurtosis, the fourth central moment, is a measure of how outlier-prone a distribution is. The kurtosis of the normal distribution is 3. Distributions that are more outlier-prone than the normal distribution have kurtosis greater than 3; distributions that are less outlier-prone have kurtosis less than 3.

The skewness and kurtosis, averaged across the 11 users, of the feature distributions for the four spectral methods are given in Table III. "Top" indicates the distribution for the upper target and "Bottom" indicates the distribution for the lower target. Table III shows that the matched filter generally produces features that are more Gaussian than the other methods and, thus, should presumably result in better cursor control. The same effect can be achieved by applying a simple normalizing transformation to the distributions of the other methods [2]. However, this transformation is not entirely trivial if the underlying prespectral analysis distribution is not Gaussian, which is not assumed in this case. The considerable differences in skewness and kurtosis between target locations can be attributed to burstiness of the μ rhythm in the synchronized condition, as mentioned earlier.

IV. ONLINE RESULTS

The parameterized μ-matched filter (MF) was implemented to generate features for online cursor control in BCI2000 [15]. Data were collected from 4 of the available users that participated in the offline analysis (2 male and 2 female, users A, D, F, and K) to compare the μ-matched filter and the incumbent 16th-orfer AR spectral analysis (AR1). Using the same protocol described earlier, the users again performed the one-dimensional cursor control task. Each user completed 4 sessions consisting of 8 runs using the AR1 and MF methods alternating in blocks of 4 runs in a counterbalanced fashion. Because the individualized analysis was not conducted at the time of the online sessions, the MF model parameters were fixed at $a_2/a_1 : a_3/a_1 = [0.26 : 0.08]$ and $\phi_2 : \phi_3 = [\pi : 0]$ for all users based on the template derived in [5], using the individual fundamental frequencies. Although these fixed model parameters were not optimal in all cases, the resulting template waveforms were nonetheless very similar to the characteristic waveforms. The online results are summarized in Fig. 6. A repeated measures ANOVA on the online run results using METHODS, USERS, and RUNS as factors. The ANOVA indicates a statistically significant ($F(1, 3) = 6.75$, p $= 0.0105$) improvement in performance using the μ-matched filter. However, there also is a significant interaction between the methods and the users ($F(3, 9) = 4.19$, p $= 0.0074$), which was not the case in the offline analysis and can be attributed to the use of suboptimal parameters online. Nevertheless, the results demonstrate the efficacy of the MF in general, and it is expected that the performance should be further improved with the individualized model parameters obtained from the characteristic waveforms.

V. DISCUSSION

The offline analyses indicate that a single matched filter feature is able predict the target as well or better than two μ and β features derived from the AR and FFT spectral bins. This suggests that the μ and β bands often demonstrate a consistent amplitude/phase relationship that is unique to a particular user, and that these bands are not entirely independent when the user is engaged in controlling the cursor. The persistence of this relationship begets the characteristic μ-rhythm morphology, which is correlated with cursor control and can be accurately estimated by the matched filter in a compact fashion. Additionally, compared to the features derived by the other feature extraction methods, the matched filter features generally have raw distributions that are less skewed and more Gaussian. This contributes
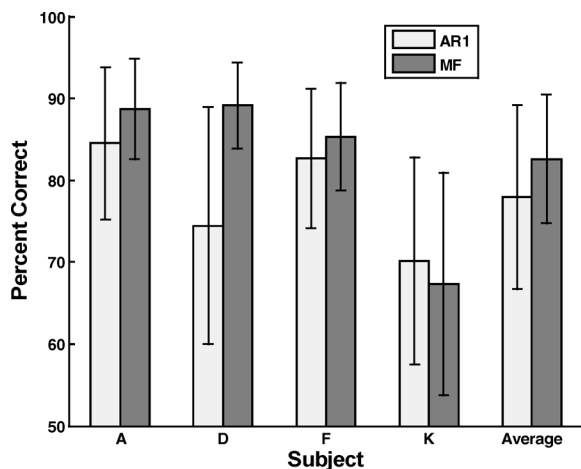
Fig. 6. Online performance of 4 of the 11 users from the offline analysis using AR (AR1) and MF features. The error bars indicate the standard deviation of the 16 runs.

to the superior performance of the matched filter in the online experiments.

The online results suggest that the μ-matched filter outperforms the incumbent AR method for feature extraction in the one-dimensional cursor control task. Also, performance with the matched filter was more consistent in general as indicated by the standard deviations in Fig. 6. Aside from the aforementioned favorable characteristics of the feature distribution, there are several possible reasons for this improved performance. Since the matched filter theoretically provides the optimal signal-to-noise ratio, the μ-matched filter is not as prone to the extraneous signal contamination that could potentially affect the other methods, especially parametric methods such as AR modeling. Furthermore, the matched filter is apt to provide a better discrimination between the μ rhythm and the more sinusoidal visual α rhythm occupying the same frequency band. This is not the case for the AR and FFT methods which merely resolve purely sinusoidal components. Similarly, the μ-matched filter is also capable of discriminating the α-asynchronous β components that may not contribute to μ-band control.

Historically, users who are able to attain consistent and accurate one- and two-dimensional cursor control seem to exhibit and actively modulate a pervasive μ-rhythm morphology over one or both hemispheres of the sensorimotor cortex. Because the μ-matched filter is able to more accurately detect and track such a control signal using fewer features, it is hypothesized that the improved one-dimensional performance will translate into improved multidimensional cursor control. Additionally, by producing fewer, better representative control features and eliminating the individual, correlated μ- and β- band features, the μ-rhythm matched filter analysis would greatly simplify and enhance the efficacy of a feature weight adaptation scheme, potentially further increasing online BCI performance.

REFERENCES

[1] M. Akin and M. K. Kiymik, "Application of periodogram and AR spectral analysis to EEG signals," *J. Med. Syst.*, vol. 24, no. 4, pp. 247–256, 2000.

[2] T. Gasser, P. Bacher, and J. Mocks, "Transformations towards the normal distribution of broad band spectrum parameters of the EEG," *Electroencephalogr. Clin. Neurophysiol.*, vol. 53, pp. 119–124, 1982.

[3] B. H. Jansen, J. R. Bourne, and J. W. Ward, "Autoregressive estimation of short segment spectra for computerized EEG analysis," *IEEE Trans. Biomed. Eng.*, vol. 28, pp. 630–8, Sep. 1981.

[4] J. Kalcher and G. Pfurtscheller, "Discrimination between phase-locked and nonphase-locked event-related EEG activity," *Electroenceph. Clin. Neurophysiol.*, vol. 94, pp. 381–384, 1995.

[5] D. J. Krusienski, G. Schalk, D. J. McFarland, and J. R. Wolpaw, "Tracking of the mu rhythm using an empirically derived matched filter," in *Proc. 2nd Int. IEEE EMBS Conf. Neural Eng.*, Mar. 16–19, 2005, pp. 86–89.

[6] W. N. Kuhlman, "EEG feedback training of epileptic patients: Clinical and electroencephalographic analysis," *Electroencephalogr. Clin. Neurophysiol.*, vol. 45, pp. 699–710, 1978.

[7] S. L. Marple, *Digital Spectral Analysis with Applications*. Englewood Cliffs, NJ: Prentice-Hall, 1987.

[8] D. J. McFarland, L. M. McCane, S. V. David, and J. R. Wolpaw, "Spatial filter selection for EEG-based communication," *Electroencephalogr. Clin. Neurophysiol.*, vol. 103, pp. 386–394, 1997.

[9] D. J. McFarland, W. A. Sarnacki, and J. R. Wolpaw, "Brain-computer interface (BCI) operation: Optimizing information transfer rates," *Biological Psychol.*, vol. 63, pp. 237–251, 2003.

[10] D. J. McFarland and J. R. Wolpaw, "EEG-based communication and control: Speed-accuracy relationships," *Appl. Psychophysiol. Biofeedback*, vol. 28, pp. 217–231, 2003.

[11] E. Niedermeyer and F. L. da Silva, Eds., Electroencephalography: Basic Principles, Clinical Applications and Related Fields 5th ed. Baltimore, MD, Williams & Wilkins, 2004.

[12] V. V. Nikulin and T. Brismar, "Phase synchronization between alpha and beta oscillations in the human electroencephalogram," *Neuroscience*, vol. 137, pp. 647–657, 2005.

[13] G. Pfurtscheller and F. H. L. da Silva, "Event-related EEG/MEG synchronization and desynchronization: Basic principles," *Clin. Neurophysiol.*, vol. 110, pp. 1842–1857, 1999a.

[14] M. G. Rosenblum, A. S. Pikovsky, J. Kurths, C. Schäfer, and P. Tass, "Phase synchronization: From theory to data analysis," in *Handbook of Biological Physics*, F. Moss and S. Gielen, Eds. Amsterdam, The Netherlands: Elsevier Science, Neuro-informatics, 2001, vol. 4, pp. 279–321.

[15] G. Schalk, D. J. McFarland, T. Hinterberger, N. Birbaumer, and J. R. Wolpaw, "BCI2000: A general-purpose brain-computer interface (BCI) system," *IEEE Trans Biomed. Eng.*, vol. 51, no. 6, Jun. 2004.

[16] F. Sharbrough, C. E. Chatrian, R. P. Lesser, H. Luders, M. Nuwer, and T. W. Picton, "American electroencephalographic society guidelines for standard electrode position nomenclature," *J. Clin. Neurophysiol.*, vol. 8, pp. 200–202, 1991.

[17] G. Turin, "An introduction to matched filters," *IEEE Trans. Inf. Theory*, vol. 6, no. 3, pp. 311–329, Jun. 1960.

[18] J. R. Wolpaw, N. Birbaumer, D. J. McFarland, G. Pfurtscheller, and T. M. Vaughan, "Brain-computer interfaces for communication and control," *Clin. Neurophysiol.*, vol. 133, pp. 767–791, 2002.

[19] J. R. Wolpaw and D. J. McFarland, "Multichannel EEG-based brain-computer communication," *Electroencephalogr. Clin. Neurophysiol.*, vol. 90, no. 6, pp. 444–9, Jun. 1994.

[20] J. R. Wolpaw and D. J. McFarland, "Control of a two-dimensional movement signal by a noninvasive brain-computer interface in humans," *Proc. Nat. Acad. Sci. USA* (Epub 2004), vol. 101(51), pp. 17849–54, Dec. 21, 2004.

Dean J. Krusienski (M'01) received the B.S.E.E., M.S.E.E., and Ph.D.E.E. degrees from The Pennsylvania State University, University Park, PA, in 1999, 2001, and 2004, respectively.

He completed his postdoctoral research at the New York State Department of Health's Wadsworth Center, Albany, NY. He is currently a Visiting Assistant Professor of Electrical Engineering at the University of North Florida, Jacksonville, where he is researching the application of adaptive signal processing and pattern recognition techniques to a non-invasive brain-computer interface that allows individuals with severe neuromuscular disabilities to operate a communication device via the EEG. His research interests include brain-computer interfaces, adaptive filtering, evolutionary algorithms, biomedical signal processing, computational intelligence, neural networks, and blind source separation.

Gerwin Schalk (M'04) received the M.S. degree in electrical engineering and computer science from Graz University of Technology, Graz, Austria, in 1999 and the M.S. degree in information technology from Rensselaer Polytechnic Institute, Troy, NY, in 2001.

He is a Research Scientist and Chief Software Engineer at the Laboratory of Nervous System Disorders, Wadsworth Center, New York State Department of Health, Albany.

His research interests include the future development of brain-computer interface technology as well as scientific and economic aspects of technology innovation.

Jonathan R. Wolpaw received the A.B. degree from Amherst College, Amherst, MA, in 1966 and the M.D. degree from Case Western Reserve University, Cleveland, OH, in 1970, and completed fellowship training in neurophysiology at the National Institutes of Health.

He is Chief of the Laboratory of Nervous System Disorders and a Professor at the Wadsworth Center, New York State Department of Health and the State University of New York, Albany. His research interests include use of operant conditioning of spinal reflexes as a new model for defining the plasticity underlying a simple form of learning in vertebrates and development of EEG-based communication and control technology for people with severe motor disabilities.

Dennis J. McFarland received the Ph.D. degree from the University of Kentucky, Lexington, in 1978.

He is currently a Research Scientist at the Wadsworth Center, New York State Department of Health, Albany. His research interests include development of EEG-based communication and analysis of auditory processing.